ResearchGate

See discussions, stats, and author profiles for this publication at: https://www.researchgate.net/publication/265213439

Prototropic Transformation and Rotational–Relaxation Dynamics of a Biological Photosensitizer Norharmane inside Nonionic Micellar Aggregates

ARTICLE *in* THE JOURNAL OF PHYSICAL CHEMISTRY B · SEPTEMBER 2014

Impact Factor: 3.3 · DOI: 10.1021/jp5056717 · Source: PubMed

CITATIONS
3

READS
61

3 AUTHORS:

Bijan Kumar Paul
Indian Institute of Science Education and Res…
72 PUBLICATIONS **896** CITATIONS
SEE PROFILE

Narayani Ghosh
Indian Institute of Science Education and Res…
10 PUBLICATIONS **22** CITATIONS
SEE PROFILE

Saptarshi Mukherjee
Indian Institute of Science Education and Res…
49 PUBLICATIONS **639** CITATIONS
SEE PROFILE

Available from: Narayani Ghosh
Retrieved on: 02 February 2016

THE JOURNAL OF PHYSICAL CHEMISTRY B

Article

pubs.acs.org/JPCB

Prototropic Transformation and Rotational−Relaxation Dynamics of a Biological Photosensitizer Norharmane inside Nonionic Micellar Aggregates

Bijan K. Paul,* Narayani Ghosh, and Saptarshi Mukherjee*

Department of Chemistry, Indian Institute of Science Education and Research Bhopal, Indore By-Pass Road, Bhauri, Bhopal 462066, Madhya Pradesh, India

Supporting Information

ABSTRACT: The effect of variation of the size of headgroup as well as the length of hydrocarbon tail of nonionic surfactants on the photophysics and rotational-relaxation dynamics of a promising biological photosensitizer, norharmane, (NHM) has been investigated. The series of nonionic micelles employed for the study belongs to Triton X family (allowing the variation in poly(ethylene oxide) (PEO) chain length) and Tween family (providing access to vary the alkyl chain length of the surfactant tails). The spectral deciphering of the photophysics of the drug (NHM) within the series of the nonionic micelles reveals remarkable influence of binding of the drug with the micelles on the prototropic equilibrium which is notably favored toward the neutral species of the drug over the cationic counterpart. The strength of drug−micelle binding interaction as well as the extent of transformation of the cation ⇌ neutral prototropic equilibrium is found to be enormously governed by the variation of the headgroup size and the alkyl chain length of the surfactants. To this end, the equilibrium constant (K_{eq}) and free energy change (ΔG) for cation ⇌ neutral prototropic transformation of the drug as a function of the micellar parameters have been meticulously explored from emission studies and comprehensively rationalized under the provision of the micellar hydration model, that is, the differential extents of water penetration to micellar units as a function of varying thickness of the palisade layer and hence a variation in the polarity of the micellar microenvironments. The significant enhancement in steady-state fluorescence anisotropy of NHM in micellar environments compared to that in bulk aqueous buffer phase substantiates the location of the drug in motionally constrained regions introduced by the nonionic micelles. Further, all these lines of arguments are effectively corroborated from time-resolved fluorescence experiments with particular emphasis on time-resolved anisotropy decay study of the drug within the micellar aggregates.

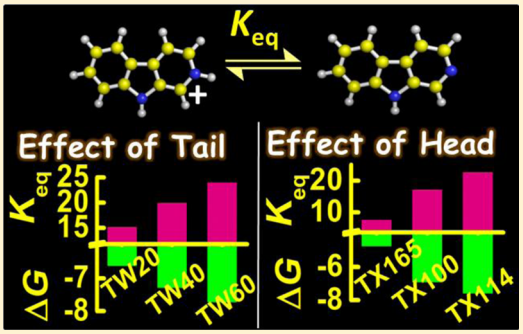

1. INTRODUCTION

The interaction and the associated photophysics of various organic compounds when trapped inside self-organized assemblies, like micelles, reverse-micelles, vesicles, cyclodextrins, etc., have been well documented in the literature.[1−11] Additionally, the conspicuous thrust of research activities surrounding such self-organized assemblies is also originating from their promising applications in some of the modern day requirements, such as development of energy storage devices, nanometer sized electronic devices, and targeted drug delivery.[12,13] Among the various self-organized assemblies, micellar systems occupy a seminal position and have been a topic of contemporary research for many years.[1−13] Surfactant molecules, which are amphiphilic in nature, self-aggregate to form micelles at a specific concentration of the surfactant which is termed as the critical micelle concentration (CMC). Owing to their unique ability to function as a comprehensive, simple model mimicking biological membranes, micellar systems have been thoroughly investigated and have attracted considerable research interests for many years.[8,9] Compared to the complex biological systems, micellar systems are generally optically transparent and scatter free. Thus, they can be easily studied by using several spectroscopic techniques. The study of interaction of small molecules with micellar systems are of fundamental importance as they provide a molecular level understanding regarding the associated noncovalent intermolecular forces.[1]

In the present manuscript, we have thoroughly investigated the interaction of a potent cancer cell photosensitizer, β-carboline with a series of nonionic micellar systems. β-Carbolines are naturally occurring alkaloids having tremendous biological significances and have found enormous applications in medical sciences.[14−20] They serve as monoamine-oxidase enzyme inhibitors, interact with neurotransmitters and neuromodulators of the central nervous system,[14−16] and are often used in photodynamic therapy where they exhibit the role of photosensitizers.[17−20] Thus, the large spectrum of applications, mainly related to their biological properties, have naturally triggered the inquisition toward investigating their interactions with biomi-

Received: June 7, 2014
Revised: August 2, 2014
Published: September 1, 2014

ACS Publications © 2014 American Chemical Society

dx.doi.org/10.1021/jp5056717 | J. Phys. Chem. B 2014, 118, 11209−11219

metic systems and drug delivery vehicles.[21,22] To this end, micellar systems have shown promising prospects in solubilization and carrying of drugs, and their subsequent transport to specific targeted sites. The ability of micellar assemblies to noncovalently bind to numerous organic compounds has also led to their application in biodetoxification of drugs from the body. Our present work explores the interaction of norharmane (NHM, Scheme 1) with a series of nonionic micellar assemblies varying in their headgroup size and the tail length of the surfactant molecules.

Scheme 1. (a) Schematic Representation of the Prototropic Equilibrium of NHM, (b) Structures of Tween, and (c) Structures of Triton X Surfactants

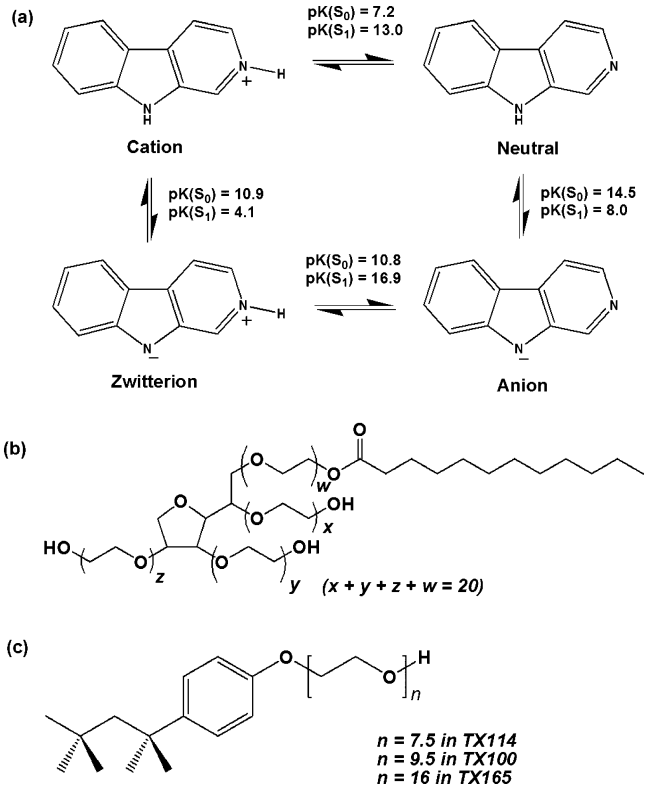

Although a plethora of works mainly focusing on the structural aspects of nonionic micelles, like variation of size, shape, and hydration of the micelles as a function of the poly(ethylene oxide) (PEO) and alkyl chain length have been well documented,[23,24] discussions related to the water-micelle interactions still remain sparse in the literature. Herein, we try to unravel how the interaction of the bioactive drug molecule, NHM with nonionic micellar systems varies with the PEO chain lengths and alkyl chain lengths of the surfactant molecules. The microheterogeneous environment which a drug molecule experiences when encapsulated within a complex biological system is well understood from knowledge of the rotational dynamics of the drug molecule. When a fluorophore is entrapped in a constrained environment, its rotational motions are fundamentally different from what is encountered in a bulk media because of the motional restrictions thereby imparted on the fluorophore molecules. Hence, besides characterizing the drug-micelle interactions, the present work emphasizes on the various microheterogeneous environments the drug molecule experiences by estimating the rotational-relaxation dynamics of the drug within the micelle-encapsulated state.

For the above stated purposes, we have rationally chosen two separate series of nonionic micelles, namely, the Triton X series (which allows variation in PEO chain length) and the Tween series (which allows the variation in alkyl chain length) (Scheme 1). The surfactants belonging to the Triton X family contain a *p-tert*-octylphenyl (OP) hydrophobic moiety with a varying poly(ethylene oxide) (PEO) unit comprising the hydrophilic part.[25] The Triton X series employed in the present study are Triton X-165, Triton X-100, and Triton X-114 having 16, 9.5, and 7.5 units of PEO, respectively. The surfactants of the Tween family are constituted of 20 poly(ethylene oxide) hydrophilic headgroups having different alkyl chain lengths. The presently employed Tween series of surfactants are Tween 20, Tween 40, and Tween 60 having carbon chain lengths of 12, 16, and 18, respectively.

2. EXPERIMENTAL SECTION

2.1. Materials. Norharmane (NHM, Scheme 1) and all the surfactants from the Triton X (TX) series (namely, TX165, TX100, and TX114), and the Tween (TW) series (namely, TW20, TW40, and TW60) procured from Sigma-Aldrich, USA were used as received without any further purification. Tris buffer was also procured from Sigma-Aldrich, USA and 0.01 M Tris–HCl buffer of pH 7.4 was prepared in deionized triply distilled Milli pore water. Hydrochloric acid (HCl) was used as supplied from Finar Scientific, India.

2.2. Instrumentations and Methods. *Steady-State Measurements.* The absorption and fluorescence (emission and excitation) spectra were recorded on a Carry 100 UV–vis spectrophotometer and HORIBA JOBIN YVON Fluorolog 3–111 fluorometer, respectively. All spectroscopic studies are performed with appropriate background corrections using freshly prepared solutions having a low concentration of NHM (~2.0 μM) in order to minimize the inner filter effects. The experimental spectra have been deconvoluted into individual Gaussian curves using the Marquardt–Levenberg algorithm as implemented in MS Origin 7 following the procedure reported elswhere.[26]

Steady-state anisotropy (r) was recorded on a HORIBA JOBIN YVON Fluorolog 3–111 fluorometer. The steady-state anisotropy (r) is defined as[27]

$$r = \frac{I_{VV} - GI_{VH}}{I_{VV} + 2GI_{VH}} \quad (1)$$

where, I_{VV} is the fluorescence intensity when both the excitation and emission polarizers are oriented vertically, and I_{VH} is the fluorescence intensity when the excitation polarizer is vertically and the emission polarizer is horizontally oriented. The correction factor, G is given by

$$G = \frac{I_{HV}}{I_{HH}} \quad (2)$$

Time-Resolved Measurements. For fluorescence lifetime measurements, the samples were excited at 378 nm (IBH-NanoLED-375L having a typical full width at half-maximum ~90 ps) and 340 nm (IBH-NanoLED-340 having a typical full width at half-maximum ~800 ps) using picosecond diode sources. The emission was collected at magic angle polarization[28] using a Hamamatsu MCP Photomultiplier (Model R-3809U-50). The time-correlated single photon counting (TCSPC) set up consists

dx.doi.org/10.1021/jp5056717 | J. Phys. Chem. B 2014, 118, 11209–11219

of an Ortec 9327 pico-timing amplifier. The data was collected with a PCI-6602 interface card as a multichannel analyzer.

The time-resolved fluorescence anisotropy decay function, $r(t)$ is given as[27,28]

$$r(t) = \frac{I_{\parallel}(t) - GI_{\perp}(t)}{I_{\parallel}(t) + 2GI_{\perp}(t)} \quad (3)$$

where, $I_{\parallel}(t)$ and $I_{\perp}(t)$ designate fluorescence decays obtained for parallel and perpendicular emission polarizations, respectively, with respect to the vertical excitation polarization, and G, the grating factor was determined from long time tail matching technique.[28]

Dynamic Light Scattering. Dynamic Light Scattering (DLS) experiments were carried out using Beckman Coulter Delsa Nano C instrument, employing a 5 mW, 633 nm He−Ne laser and equipped with a thermostated sample chamber. The experimental data were processed using the supplied instrumental software to estimate the hydrodynamic radii (r_h) of the various micellar systems under investigation.

3. RESULTS AND DISCUSSION

3.1. Spectroscopic Analysis of the Drug (NHM)−Micelle Interaction. The fluorophore NHM exhibits two distinct absorption bands centered at ∼340 nm and ∼370 nm in aqueous buffer. According to literature reports,[14−16,19−22,29−35] these two absorption bands are ascribed to the neutral and cationic species of NHM (Scheme 1), respectively. The β-carboline systems (e.g., NHM) are well-known to undergo tautomeric equilibria in aqueous medium as a function of the medium pH.[14−16,19−22,29−35] The presence of different types of nitrogen atoms (namely, pyridinic and pyrrolic nitrogen atoms) within the same molecule is often invoked to lead to considerably different electronic charge density modulations on them following photoexcitation. This leads to inherently complicated pH-dependent prototropic equilibria in these compounds in the ground as well as excited-states.[14,19−21,33−35] Again it is well reported that acid−base equilibrium of a compound is also sensitive to solvent properties like the polarity, dielectric constant etc.[14,19−21,33−35] The medium polarity-dependent prototropic activities of β-carboline and some of its derivatives have been reported in the literature[14−16,19−22,29−35] and also found in the present investigation with NHM as described in a forthcoming discussion (Section 3.5). The representative absorption and emission spectral properties of NHM in aqueous solution as a function of medium pH as displayed in Figure S1 of the Supporting Information are found to be in good agreement with reported literatures.[14−16,19−22,29−35] In aqueous solution at acidic pH, NHM yields absorption band for the cationic species. The transformation from the cationic to the neutral species in alkaline pH is characterized by a blue-shift in the absorption profile, whereas at neutral pH (pH = 7.2), the absorption profile of NHM is designated by band features which are typical of both the neutral and cationic species as exemplified by Figure S1a.[14−16,19−22,29−35] The fluorescence emission spectra of NHM in medium of varying pH are displayed in Figure S1b. As seen in the figure and also supported by previous studies,[19−22,29−35] the representative emission profiles of NHM are found to yield only the characteristic emission for the cationic species (λ_{em} ∼ 450 nm) in aqueous solution in the pH range 1−10. However, in highly alkaline pH (pH ∼ 12.0−13.0) the emission profile reflects the signature from all the three prototrpoic species, namely, neutral, cation and zwitterion. In order to enable a clearer visual perusal, the experimental fluorescence spectrum of NHM at pH 12.3 has been deconvoluted into individual Gaussian components which show distinct features of the resolved bands conforming to emission from neutral, cationic, and zwitterionic species of NHM which is in excellent agreement with the experimental emission profile. Similar resolution of the experimental spectra obtained in the range pH 1−10 produced only the characteristic emission of the cationic species (λ_{em} ∼ 450 nm) of NHM, in excellent accord with reported literatures.[14−16,19−22,29−35]

The absorption profile of NHM undergoes significant modification following interaction with the micellar systems. Incremental addition of the nonionic surfactants to an aqueous buffer solution of NHM accompanies enhancement of absorbance of the neutral band (λ_{abs} ∼ 340 nm) with concomitant reduction of the cationic counterpart (λ_{abs} ∼ 370 nm) as shown in Figure 1 for the representative cases of TW20

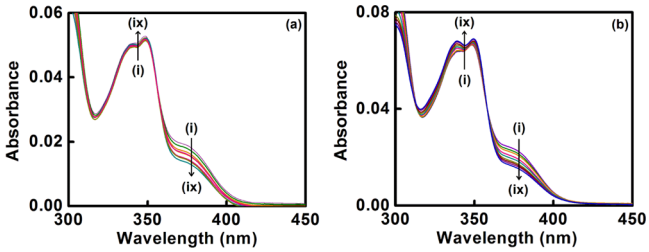

Figure 1. Absorption profile of the drug NHM with added (a) TW20, and (b) TX165. Curves i → ix correspond to [TW20] = 0, 0.025, 0.12, 0.25, 0.38, 0.50, 0.62, 0.75, 1.0 mM in part a and [TX165] = 0, 0.25, 0.5, 1.0, 1.5, 2.0, 2.5, 3.0, 3.25 mM in part b.

and TX165. These findings readily evince that the prototropic equilibrium of NHM (Scheme 1) is remarkably modified within the micellar environments as compared to that in aqueous buffer phase.[14−16,19−22,29−35] Thus, from the absorption spectra, we can conclude that the prototropic transformation of NHM in the ground-state favors the neutral species over the cationic counterpart within the micellar assemblies. Consequently, the prototropic equilibrium of NHM is affected by a decrease in the polarity of the medium of the drug binding site under investigation.

In aqueous buffer solution, NHM exhibits an emission maximum centered at ∼450 nm which is a clear signature of the presence of the cationic species.[14−16,19−22,29−35] As displayed in Figures 2 and 3, the emission profile of NHM undergoes remarkable modification upon interaction with the studied micellar systems. The cationic fluorescence band of NHM (λ_{em} ∼ 450 nm) undergoes significant quenching, alongside the development of a new emission band at λ_{em} ∼ 380 nm originating from the neutral species of NHM (Scheme 1).[14−16,19−22,29−35] The cationic fluorescence band of NHM also undergoes a small blue-shift within the micelles as compared to that in aqueous buffer phase (Figures 2 and 3) indicating that the probe NHM experiences a more hydrophobic environment within the micellar units as compared to bulk phase.

Further, the experimentally obtained emission spectra of NHM in various environments have been subjected to component analysis by resolving into individual Gaussian curves which enables a distinct perusal of the characteristic emission band features arising from various prototropic species of the drug. As seen from Figure 4a, upon deconvolution, the emission spectrum of NHM in aqueous buffer conforms to only one band

dx.doi.org/10.1021/jp5056717 | J. Phys. Chem. B 2014, 118, 11209−11219

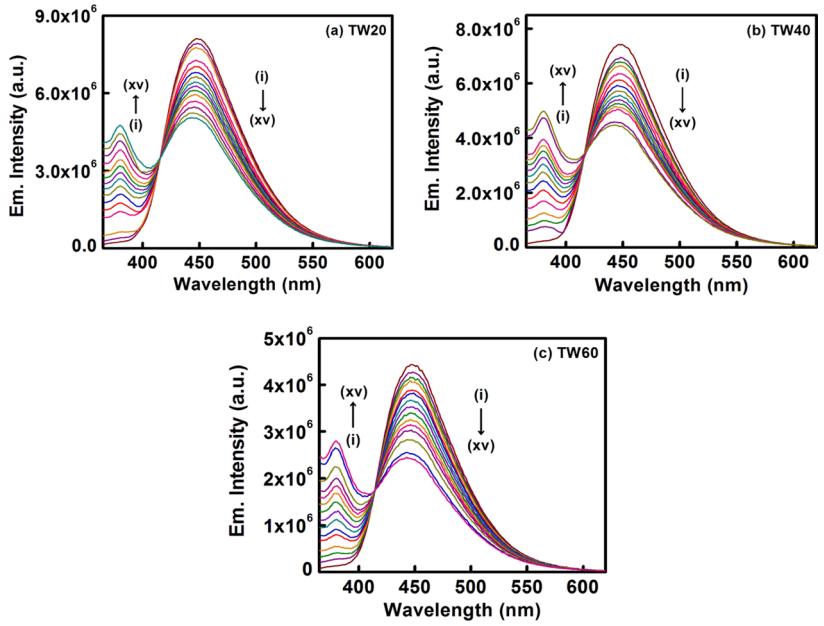

Figure 2. Emission spectra of the drug NHM with added (a) TW20, (b) TW40, and (c) TW60 in aqueous buffer medium. Curves i → xv correspond to [TW20] = 0, 0.025, 0.062, 0.12, 0.19, 0.25, 0.31, 0.38, 0.44, 0.50, 0.56, 0.62, 0.75, 0.88, 1.0, 1.12 mM in part a, [TW40] = 0, 0.062, 0.088, 0.12, 0.19, 0.25, 0.31, 0.38, 0.44, 0.50, 0.56, 0.62, 0.69, 1.0 mM in part b, and [TW60] = 0, 0.024, 0.048, 0.071, 0.12, 0.14, 0.19, 0.24, 0.30, 0.36, 0.42, 0.48, 0.59, 0.83, 0.95 mM in part c.

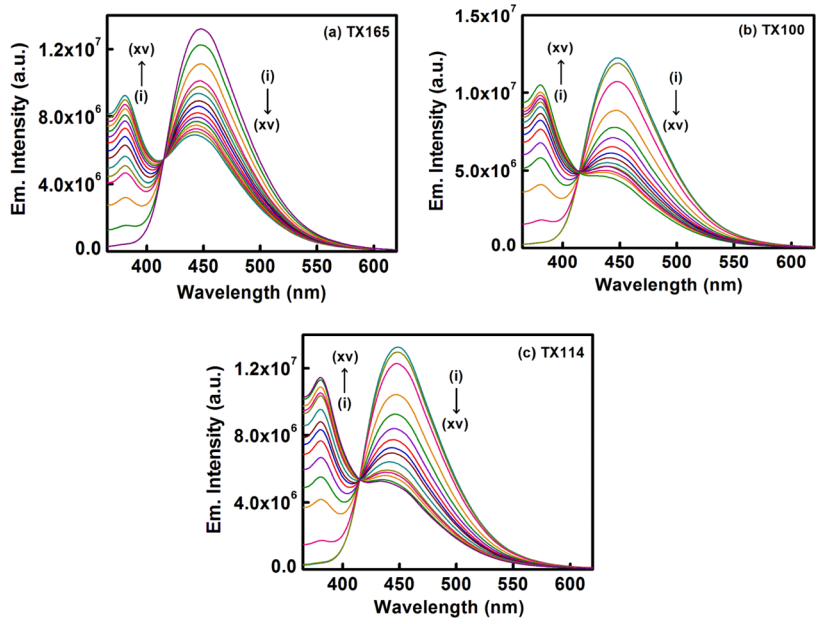

Figure 3. Emission spectra of the drug NHM with added (a) TX165, (b) TX100, and (c) TX114 in aqueous buffer medium. Curves i → xv correspond to [TX165] = 0, 0.25, 0.5, 0.75, 1.0, 1.25, 1.5, 1.75 2.0, 2.25, 2.5, 2.75, 3.0, 3.25, 3.5 mM in part a, [TX100] = 0, 0.25, 0.5, 0.75, 1.0, 1.25, 1.5, 1.75, 2.0, 2.25, 2.5, 2.75, 3.0, 3.25, 3.5 mM in part b, and [TX114] = 0, 0.25, 0.5, 0.75, 1.0, 1.25, 1.5, 1.75, 2.0, 2.25, 2.5, 2.75, 3.0, 3.25, 3.5 mM in part c.

implying the presence of the cationic species at $\lambda_{em} \sim 450$ nm. However, deconvolution of the emission profile of micelle (Tween and Triton X series)-bound NHM shows prominent band features corresponding to the emission of the neutral form of NHM at $\lambda_{em} \sim 380$ nm and the cationic form at $\lambda_{em} \sim 450$ nm, as depicted in Figure 4, parts b and c, for the representative cases of TW20 and TX165, respectively (the results with other surfactants in the series are compiled in the Supporting Information, Figure S2).

It could be pertinent here to note that the dynamics of structural changes of NHM following photoexcitation between the cation and neutral forms may also involve a zwitterion (Scheme 1). The spectroscopic signature of the zwitterionic species of NHM has been found to emerge at pH 12−13 as a characteristic emission band feature at $\lambda_{em} \sim 510$ nm, as stated earlier (Figure S1 in the Supporting Information), in consensus with a score of previous studies on NHM and a variety of analogous β-carboline derivatives.[14−16,19−22,29−35] According to Reyman et al.,[33] the fluorescence decay behavior of the zwitterionic species can be probed by monitoring the time-resolved fluorescence decay transient of NHM at pH 12.3 at $\lambda_{em} \sim 540$ nm, Figure S3 and Table S1 in the Supporting

dx.doi.org/10.1021/jp5056717 | J. Phys. Chem. B 2014, 118, 11209−11219

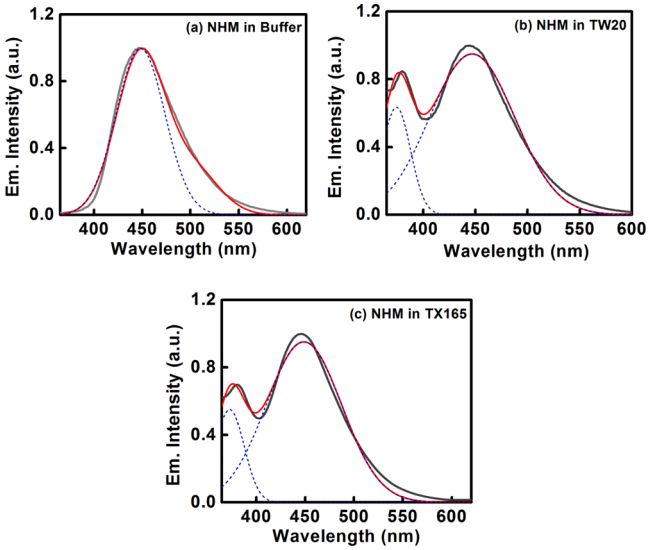

Figure 4. Resolved emission spectra of NHM in (a) aqueous buffer solution, (b) TW20 (1.0 mM), and (c) TX165 (2.0 mM). The bold gray lines denote the experimental spectra, the blue dotted lines denote the resolved bands into the individual Gaussian components, and the red lines designate the simulated spectra based on the resolved bands.

Information. In tune with reported literatures,[14−16,19−22,29−35] the fluorescence decay of NHM at pH 12.3 (λ_{em} ~ 540 nm) is found to be aptly described by a biexponential decay pattern with a fast component having a negative pre-exponential factor (Table S1 of the Supporting Information) which indicates the formation of the zwitterion from the cation in the excited-state.[19,33,35] On the basis of this information, we were driven by the inquisition to delve into the possibility of formation of the zwitterionic species of NHM in the micellar environments. In order to resolve the issue, we have banked upon the protocol of directly comparing the present experimental results with those observed during formation of the zwitterion. To this end, the following lines of arguments are advocated:

(i). Steady-State Emission Spectral Study. In order to evaluate the emission characteristics of the zwitterionic species of NHM (λ_{em} ~ 510 nm, Figure S1 in the Supporting Information) in the presence of the nonionic micellar units the experimental fluorescence emission profile of the micelle-bound NHM has been deconvoluted into three individual Gaussian components describing the characteristics of the three prototropic species, namely, neutral (λ_{em} ~ 380 nm), cation (λ_{em} ~ 450 nm), and zwitterion (λ_{em} ~ 510 nm). As illustrated in Figure S4 of Supporting Information, the resolution of the experimental spectral profiles in the presence of all the nonionic surfactants investigated into individual Gaussian curves yields spectral signatures typical of the exclusive presence of the neutral and the cationic species of NHM, and not the zwitterionic species within the as-employed experimental window.

Furthermore, it is noted that the cation ⇌ neutral prototropic transformation of NHM within the micellar environments is characterized by a distinct isoemissive point (Figures 2 and 3), which in turn endorses the spectroscopic signature for the fact that the prototropic equilibrium of NHM is restricted within the two species, in excellent congruity to the aforementioned results.

(ii). Medium pH. All the experiments have been conducted in aqueous buffer solution (pH 7.4) which is expected to maintain the pH of the medium in the course of the experiments, whereas the zwitterionic emission of NHM is observed in the pH range of 12−13, Figure S1 of Supporting Information. Hence it is rational to conclude that when a buffer solution is used as the medium, the equilibrium of NHM will be restricted within the two prototropic species, neutral and cation.

(iii). Time-Resolved Fluorescence Decay. The dynamics of fluorescence decay of the zwitterion (λ_{em} ~ 540 nm) is found to be characterized by a biexponential decay with a fast component having a negative pre-exponential factor (Figure S3 and Table S1 in the Supporting Information),[19,33,35] as discussed earlier. In order to entail a direct comparison in this perspective, the fluorescence decay of the micelle-bound drug has been followed under the same experimental conditions (λ_{ex} = 340 nm, λ_{em} = 540 nm), Figure S3 and Table S1 in the Supporting Information, and is found to be in excellent accord with the data recorded at λ_{em} = 450 nm following photoexcitation at λ_{ex} = 378 nm for micelle-bound NHM (Figure 10 and Table 2, as discussed later). Thus, the lack of time-resolved fluorescence decay signature characterizing the zwitterionic species of NHM within the micellar environments (λ_{em} = 540 nm, Table S1) as against the observed cogency with the decay behavior recorded at λ_{em} = 450 nm (Table 2) can be argued to corroborate to the above inferences, that is, the prototropic transformation of NHM within the micellar environments is described by the Cation ⇌ Neutral equilibrium.[19,33,35]

3.2. Cation ⇌ Neutral Prototropic Equilibrium. The basic pattern of modulation of the emission spectra of NHM, Figures 2 and 3, following interaction with all the micellar systems is qualitatively analogous within the present experimental window, though the scenario varies on close perusal of the data on a quantitative ground. To this end, the modulation of the cation ⇌ neutral prototropic equilibrium of NHM as a function of varying surfactant concentrations can be quantitatively assessed from estimation of the equilibrium constants

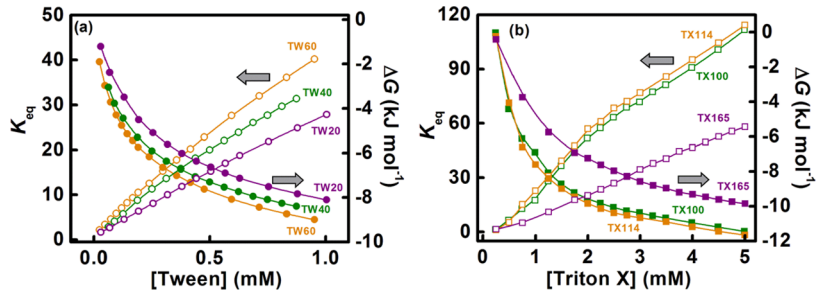

Figure 5. Variation of equilibrium constant (K_{eq}: open symbol) for the Cation ⇌ Neutral prototropic transformation of the drug (NHM) and the corresponding free energy change (ΔG: solid symbol) in different micellar environments as specified in the figure legends for (a) the Tween series and (b) the Triton X series.

dx.doi.org/10.1021/jp5056717 | J. Phys. Chem. B 2014, 118, 11209−11219

(K_{eq}) and free energy changes (ΔG). Assuming that the fluorescence intensities of the neutral and cationic species of NHM proportionately reflect the concentrations of the respective species, K_{eq} can be expressed as K_{eq} = [neutral]/[cation] = $I_{neutral}/I_{cation}$, and the associated free energy change for the process as $\Delta G = -RT \ln K_{eq}$. The variation of the K_{eq}, and ΔG as a function of surfactant concentration for both the micellar series under study are displayed in Figure 5, which shows that the prototropic equilibrium of NHM is increasingly favored toward the neutral species over the cationic counterpart. It is further noted that at the saturation of drug-micelle interaction, K_{eq} varies proportionately with the alkyl chain length of all the three Tween surfactants, that is, K_{eq} is minimum for TW20 and attains the maximum value for TW60 through TW40 being the intermediate. Accordingly, ΔG becomes more negative as the alkyl chain length of the surfactant increases, Figure 5a. Similarly, along the Triton X series of micelles, the prototropic transformation of the drug (NHM) is also favored toward the neutral species over the cationic counterpart with incremental addition of the surfactants, Figure 5b, with K_{eq} following the sequence: TX165 < TX100 < TX114 and thereby rendering ΔG to achieve its maximum negative value for TX114 and minimum negative value for TX165 through TX100. In tune with this observation, the ΔG for this prototropic transformation is found to be more negative with decreasing PEO chain length.

Qualitatively, the pattern of these observations can be compared to the fluorescence behavior of the drug with varying solvent polarity. The fluorescence behavior of NHM in a varying composition of water/1,4-dioxane mixture has been elaborately studied in this context. The fluorescence spectral profile of NHM in pure water is characterized by an unstructured emission band of the cationic species only ($\lambda_{em} \sim 450$ nm) while with decreasing polarity of the medium the cationic fluorescence intensity is progressively depleted with concomitant growth of the neutral emission at $\lambda_{em} \sim 380$ nm. In pure 1,4-dioxane, the neutral species of NHM exhibits the fluorescence exclusively ($\lambda_{em} \sim 380$ nm). Thus, the results in the micellar environments can be qualitatively argued to comply with a reduction of polarity at the drug binding site within the micellar units compared to that in the aqueous buffer.[36−39] At this juncture, the effect of variation of alkyl chain length of the surfactants within the Tween series and PEO chain length within the Triton X series can be invoked to rationalize the aforesaid observations (Figure 5) since these factors will in turn govern the modulation of the compactness of the micellar units and hence the degree of water penetration to micellar units (the micellar hydration model). According to previous reports,[40,41] the degree of water penetration within the micellar assemblies will inversely depend on the compactness of the units, that is, micelles with compact headgroups would be less vulnerable to water penetration. It has been previously reported that the compactness of the micelle headgroups varies commensurately with increasing chain length of the surfactant tail.[41] Extending this argument to our case, the increased chain length along the series TW20 < TW40 < TW60 should enhance the micellar compactness and thus making the micellar unit less susceptible toward water penetration. Consequently, reduced extent of water penetration (micellar hydration) to micelle with increased alkyl chain length should ensure a low polarity which in turn should favor the equilibrium of NHM more toward the neutral form over the cationic counterpart (Figure 5a). Following similar line of argument, the variation of K_{eq} across the Triton X series can also be annotated in the sense that increasing PEO chain length (TX114 < TX100 < TX165) accompanies a lesser degree of micellar compactness and hence a greater degree of water penetration. Thus, within the Triton X series, decreasing PEO chain length should accompany lower degree of polarity whereby favoring the cation ⇌ neutral prototropic equilibrium more toward the neutral species (along the order: TX165 < TX100 < TX114, Figure 5b).

3.3. Binding of NHM to Micelles. The NHM-micelle binding interaction can be assessed by the following equation:[30]

$$\frac{1}{I_x - I_0} = \frac{1}{I_\infty - I_0} + \frac{1}{K[M]} \times \frac{1}{I_\infty - I_0} \quad (4)$$

where, K denotes the binding constant and I_0, I_x and I_∞ represent respectively, the fluorescence intensities of NHM in the absence of surfactant, at an intermediate concentration of surfactant and under saturated conditions of interaction. In the above equation, the micellar concentration [M] can be estimated from knowledge of the concentration ([S]), CMC and aggregation number (N_{agg}) of the surfactants using the following relationship:

$$[M] = \frac{[S] - CMC}{N_{agg}} \quad (5)$$

Figures 6 and 7 display the $1/[I_x - I_0]$ vs $1/[M]$ plots for NHM in all the micellar systems studied. The binding constant (K) is

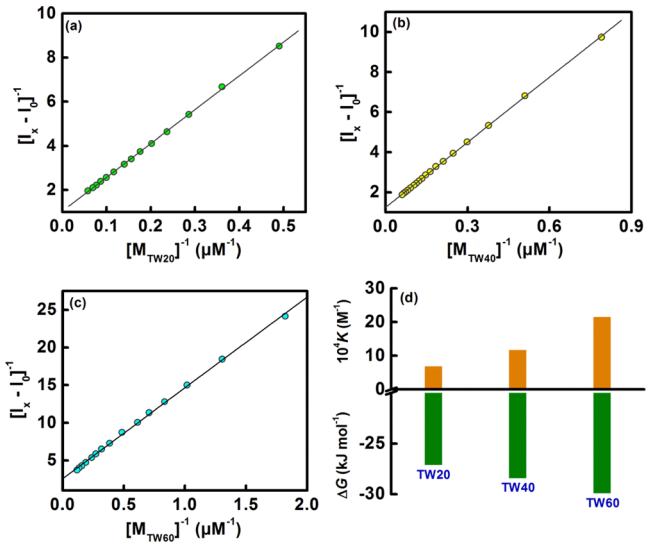

Figure 6. Double reciprocal plot of $1/[I_x - I_0]$ vs $1/[M]$ for determination of the drug (NHM)−micelle binding constant (K) for interaction of the drug with (a) TW20, (b) TW40, and (c) TW60. (d) Bar diagram showing the dependence of the drug (NHM)−micelle binding constant (K), and the corresponding free energy change ($\Delta G_{binding}$) of the interaction on the variation of the alkyl chain lengths of the surfactants used.

evaluated from the respective plots following eq 4, and the corresponding free energy change ($\Delta G_{binding}$) for the drug-micelle binding process is calculated as

$$\Delta G_{binding} = -RT \ln K \quad (6)$$

The various thermodynamic parameters are summarized in Table 1. The negative values of $\Delta G_{binding}$ clearly exemplify the fact the binding interactions of NHM with all the micellar systems are spontaneous in nature. The variation of the magnitude of the binding constants in the two different series of micellar assemblies is worth noting here, as further pictorially

dx.doi.org/10.1021/jp5056717 | J. Phys. Chem. B 2014, 118, 11209−11219

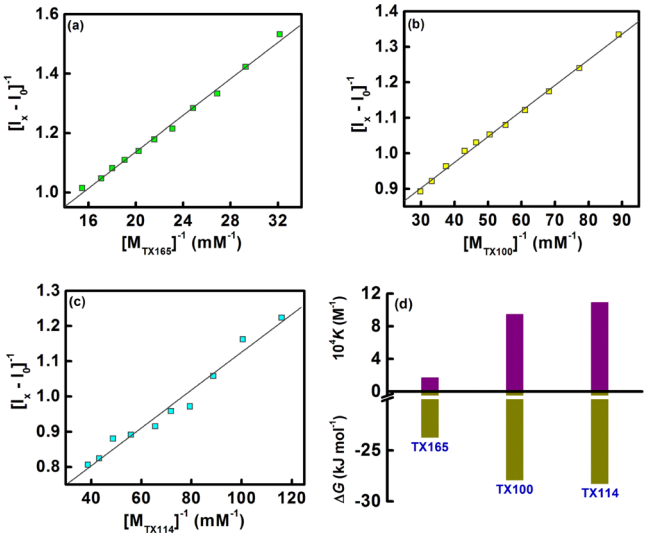

Figure 7. Double reciprocal plot of $1/[I_x - I_0]$ vs $1/[M]$ for determination of the drug (NHM)−micelle binding constant (K) for interaction of the drug with (a) TX165, (b) TX100, and (c) TX114. (d) Bar diagram showing the dependence of the drug (NHM)−micelle binding constant (K), and the corresponding free energy change ($\Delta G_{binding}$) of the interaction on the variation of the PEO chain lengths of the surfactants used.

Table 1. Binding Constants (K) and Free Energy Change (ΔG) for Drug (NHM)−Micelle Interaction, and the Micropolarity Values ($E_T(30)$) of NHM in Nonionic Micellar Environments

environment	binding constant, K (10^4 M^{-1})	ΔG (kJ mol^{-1})	$E_T(30)$ (kcal mol^{-1})
TW20	6.77	− 27.09	55.21
TW40	11.60	− 28.41	54.05
TW60	21.40	− 29.89	53.93
TX165	1.70	− 23.73	55.24
TX100	9.48	− 27.92	53.34
TX114	10.94	− 28.26	53.27

presented in panel d of Figures 6 and 7. It is evident that the drug (NHM)−micelle (Tween/Triton X) binding strength varies markedly with variation in the alkyl chain length (Tween series) and the PEO chain length (Triton X series). The magnitudes of K are found to vary inversely with the PEO chain length in case of Triton X series ($K_{TX165} < K_{TX100} < K_{TX114}$) while the variation is proportionate with the alkyl chain length in case of Tween series, that is, $K_{TW20} < K_{TW40} < K_{TW60}$ (Table 1, Figures 6d and 7d).

3.4. Steady-State Fluorescence Anisotropy. Figure 8 shows the variation of steady-state fluorescence anisotropy (r) of NHM following interaction with the surfactants. The substantial increase in r of NHM provides the signature for impartation of motional confinement on the drug molecules within the micelle-encapsulated state. A discernible increase in r of NHM is found to be gradually saturated in the higher concentration regime of the surfactants. The pattern of variation of r of NHM within the micelle-bound state is rather found to be in excellent juxtaposition with the trend of drug−micelle binding strength (section 3.3). With an increase in the length of the alkyl chain of the surfactant, the drug molecules experience an increasing degree of rigidity within the Tween series (that is, TW20 < TW40 < TW60) while the reverse trend is observed within the Triton X series (that is, increasing degree of rigidity with

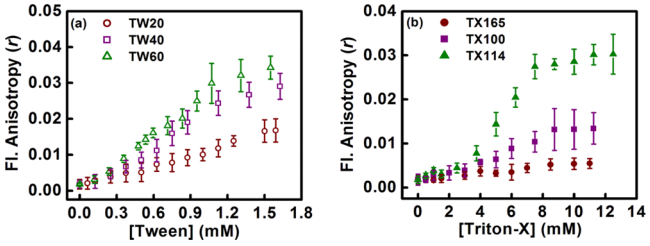

Figure 8. Variation of steady-state fluorescence anisotropy (r) of the drug (NHM) as a function of (a) Tween and (b) Triton X concentrations as specified in the figure legend. Each data point is an average of 15 individual measurements. The error bars are within the marker symbols if not apparent.

decreasing PEO chain length: TX165 < TX100 < TX114). This observation is readily understandable from consideration of the compactness in the headgroups of the studied micellar systems which varies commensurately with increasing alkyl chain length (in Tween series) and decreasing PEO chain length (in Triton X series), that is, the micellar hydration model as discussed above can be adequately applied here to rationalize the observations from steady-state fluorescence anisotropy.

3.5. Probable Location of NHM in the Micellar Aggregates. Estimating the polarity of the immediate microenvironment in and around the probe can give us valuable information regarding the probable location of the same inside the micellar units. This is generally achieved by analyzing the spectral profiles of the drug when incorporated inside the micellar units and comparing the same obtained in pure solvent(s) or solvent mixture(s) of known polarity.[7,31,32,36,37] Figure 9a depicts the fluorescence spectra of NHM as a function

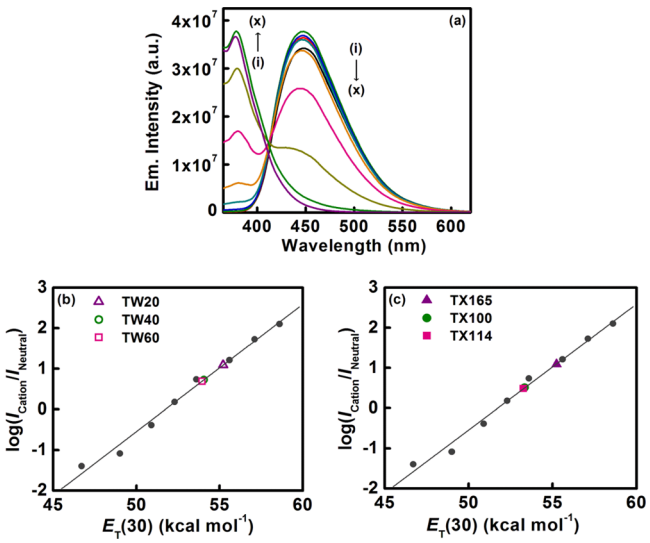

Figure 9. (a) Representative examples of modulation in emission spectral profile of the drug (NHM) in varying composition of water/1,4-dioxane mixture. Curves i → ix correspond to % 1,4-dioxane (v/v) = 0, 10, 20, 30, 40, 50, 60, 70, and 80. Panels b and c show the micropolarity values at the interaction sites of the drug in various micellar environments as specified in the figure legend. The calibration curve for micropolarity determination has been constructed by plotting the ratiometric variation of emission intensities of the cationic to neutral species of NHM ($I_{cation}/I_{neutral} = I_{450\ nm}/I_{380\ nm}$) as a function of the polarity equivalent parameter, $E_T(30)$ (in kcal mol^{-1}) of the reference water/1,4-dioxane solvent mixture.

dx.doi.org/10.1021/jp5056717 | J. Phys. Chem. B 2014, 118, 11209−11219

of medium polarity obtained by varying compositions of water/1,4-dioxane mixture. Upon decreasing the polarity of the medium, the cation fluorescence ($\lambda_{em} \sim 450$ nm) of NHM also decreases, while a new band characteristic of the neutral species is obtained at $\lambda_{em} \sim 380$ nm. This is readily understandable on the ground of increasing stabilization of the neutral species of NHM over the cationic counterpart with reduction in medium polarity.[7,31,32,36,37]

A ratiometric variation of the fluorescence intensities of the cation to neutral species, that is, $I_{cation}/I_{neutral}$, of NHM when compared to the polarity equivalent parameter, $E_T(30)$ in water/1,4-dioxane mixture is often used to estimate the immediate polarity of the drug when encapsulated inside a micellar aggregate.[36,37] Parts b and c of Figures 9 give us an estimate regarding the different polarities experienced by NHM in the micellar environments and the data are summarized in Table 1. As seen from the table, the estimated micropolarity values of NHM in different micellar environments undergo a reduction as compared to that observed in aqueous buffer ($E_T(30) = 63.1$ kcal mol^{-1}).[37] In analogy to reported literatures,[38,39] the estimated polarity values as mentioned in Table 1 closely resemble the polarity of the palisade layer of nonionic micellar system. Hence, based on such an observation, we can conclude that the probable location of NHM molecules inside the different micellar environments is the palisade layer. The estimated micropolarity values show that the environment in the near vicinity of the micelle-bound drug is most polar in TW60 and least polar in TW20 along the Tween series that is, the polarity of the drug microenvironment decreases with increasing alkyl chain length of Tween micelles while the trend is typically reversed with Triton X series micelles in which increasing PEO chain length ensures a more polar environment. The change in polarity of the drug microenvironment thus follows the order: TW20 > TW40 > TW60 within the Tween series and TX114 < TX100 < TX165 within the Triton X series (Figure 9b, c and Table 1). The observed trends rather appear tenable on the lexicon of the water penetration model into a micellar structure. The increase in alkyl chain length accompanies increasing degree of micellar compactness and thereby restricting water penetration which justifies the trend of polarity along the Tween series.[40,41] On the other hand, with increasing PEO chain length the micelle suffers a greater extent of water penetration because of reduced compactness and hence the aforementioned trend of polarity along the Triton X series micelles.[40,41] Thus, the results of polarity estimation around the microenvironment of the micelle-encapsulated drug are found to strongly substantiate the results of fluorescence anisotropy measurements as discussed in the previous section.

The technique of the ratiometric calibration scheme used herein to estimate the probable location of NHM inside the micellar aggregates is independent of the concentration of NHM and does not depend on the intensity and/or stability of the excitation source. Further, the use of water/1,4-dioxane mixture as a reference is more rational than using other solvents like methanol ($E_T(30) = 55.5$ kcal mol^{-1}) or ethanol ($E_T(30) = 51.9$ kcal mol^{-1}).[37] As evidenced from the values of $E_T(30)$ in Table 1 (which are in close proximity to those of methanol and ethanol), if solvents such as methanol and ethanol were used instead, then the small difference from the standard values would have not enabled us to scientifically differentiate the micropolarity of NHM. Hence, these advantages underline the uniqueness of our methodology in deciphering the probable location of NHM inside the Tween and Triton X micellar assemblies based on polarity measurements.

3.6. Dynamic Light Scattering. Dynamic light scattering (DLS) is an efficient tool to estimate the hydrodynamic radius (r_h) of molecular assemblies through the application of the Stokes−Einstein−Debye relationship assuming the assembly to be spherical.[42,43] The DLS profiles of the studied micellar systems is found to produce fairly monomodal distribution (figures not shown, the relevant data describing the hydrodynamic radii are represented in Table 3).[42,43] The hydrodynamic radii of the micellar units are also found to undergo only minor changes following addition of the drug thereby confirming that no appreciable perturbation of the micellar structures are brought in upon interaction with NHM.

Table 2. Time-Resolved Fluorescence Decay Parameters of the Drug (NHM) in Various Micellar Environments

environment	τ_1 (ns)	τ_2 (ns)	α_1	α_2	χ^2
aq. buffer	21.59	–	1.00	–	1.02
[TW20] (mM)					
0.25	21.74	1.92	0.92	0.08	1.05
0.50	21.6	1.96	0.75	0.15	0.99
0.75	21.39	1.83	0.67	0.23	1.01
1.0	20.76	1.71	0.62	0.28	1.08
[TW40] (mM)					
0.25	21.81	1.98	0.87	0.13	1.02
0.50	21.51	1.70	0.76	0.24	1.09
0.75	20.99	2.01	0.70	0.30	1.06
1.0	19.97	1.86	0.64	0.36	1.07
[TW60] (mM)					
0.24	21.72	1.56	0.89	0.11	1.01
0.48	21.70	1.47	0.87	0.13	1.06
0.71	21.80	1.86	0.78	0.22	1.04
0.95	21.61	1.88	0.59	0.41	1.02
[TX165] (mM)					
1.5	21.51	8.15	0.94	0.06	1.1
2.25	22.47	9.77	0.88	0.12	1.04
3.5	23.05	9.59	0.83	0.17	1.1
6.0	25.76	9.65	0.73	0.27	1.1
[TX100] (mM)					
1.5	21.78	8.47	0.96	0.04	1.1
2.25	22.19	9.57	0.91	0.09	1.1
3.0	22.55	8.29	0.87	0.13	1.1
3.5	23.41	9.19	0.81	0.19	1.1
[TX114] (mM)					
1.5	22.12	8.18	0.98	0.02	1.1
2.25	21.36	8.16	0.94	0.06	1.09
3.0	20.08	8.19	0.90	0.10	1.09

Table 3. Rotational−Relaxation Dynamical Parameters of the Drug (NHM) within the Various Micellar Systems as Obtained from Time-Resolved Fluorescence Anisotropy Decay

environment	r_0	τ_r (ns)	α_r	r_h (nm)
aq. buffer	0.10	0.132	1.0	–
TW20	0.20	1.50	1.0	4.8
TW40	0.32	1.80	1.0	5.0
TW60	0.34	2.20	1.0	8.4
TX165	0.12	0.445	1.0	3.8
TX100	0.13	0.842	1.0	4.1
TX114	0.18	0.950	1.0	4.5

dx.doi.org/10.1021/jp5056717 | J. Phys. Chem. B 2014, 118, 11209−11219

3.7. Time-Resolved Fluorescence Decay. The representative time-resolved fluorescence decay transients for NHM in TW20 and TX165 are displayed in Figure 10, and the

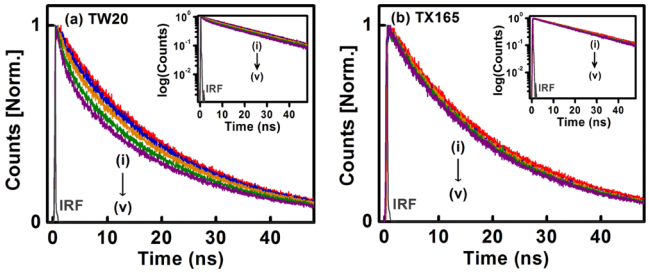

Figure 10. Typical time-resolved fluorescence decay profile of the drug (NHM) with added (a) TW20 and (b) TX165 (λ_{ex} = 378 nm, λ_{em} = 450 nm). Curves i → v correspond to [TW20] = 0, 0.25, 0.50, 0.75, 1.0 mM (a), and [TX165] = 0, 1.5, 2.25, 3.5, 6.0 mM (b). The sharp gray profile on the extreme left represents the instrument response function (IRF). The insets of each panel display the same graph on log scale.

corresponding decay parameters for all the micellar systems investigated in the present manuscript are compiled in Table 2 (the time-resolved fluorescence decay patterns of the drug in the other micellar systems are presented in the Supporting Information, Figure S5). In aqueous buffer phase, NHM exhibits an exponential decay with a lifetime of 21.59 ns.[14−16,19−22,32−35] The data summarized in Table 2 (λ_{ex} = 378 nm, λ_{em} = 450 nm) unveils that a biexponential function is required to aptly describe the fluorescence decay of the drug within the micelle-bound states. As seen from Table 2, in all the micellar systems, NHM exhibits a biexponential decay characterized by a fast and slow lifetime. The longer decay time constant (τ_1 in Table 2) is found to have striking similarity to that of NHM in bulk aqueous buffer, which is designated as the characteristic lifetime of the cationic species of NHM. The lifetime data (Table 2) clearly reveal the occurrence of two dynamical processes on distinctly different time scales (τ_1 and τ_2 in Table 2).

Inside the micellar aggregates, since the fluorescence decays of NHM display two different components, it may be argued that the slower and faster lifetimes arise from the fraction of micelle-bound and free (or unbound) drug, respectively. In this context, the validity of this proposition has been critically tested from the concept that the ratio of the relative amplitudes (pre-exponential factors), that is, α_1/α_2 should reflect the fraction of bound drug molecules to the unbound. However, calculation of the efficiency of NHM binding to the studied micellar systems following the method reported by Fayer et al.,[44] suggests that ≥99% drug molecules are actually bound to the micellar units.[21,41] This result clearly proves that the dynamics of the drug within the micellar environments is solely due to the micelle-encapsulated drug molecules with almost no significant contribution from the unbound fraction. Further, it is noted that the relative amplitude of the slower decay time constant (τ_1 in Table 2) conforming to the characteristic decay of the cationic species of NHM gradually decreases with increasing surfactant concentration. This can be related to the decreasing degree of stabilization of the cationic form of NHM over the neutral counterpart within the nonionic micelles. The present observations thus strongly corroborate to the steady-state spectral results (Section 3.1), that is, the cation ⇌ neutral prototropic equilibrium of NHM is favored more toward the neutral species within the micelle-encapsulated state.

It is known that the prototropic transformations of NHM involve different types of proton transfer reactions which would be expected to be differentially governed by various solvents. According to previous studies by Reyman et al.,[19,33,35] and others,[21,45,46] solvation has been argued to dominate the dynamics of proton transfer reactions of NHM. Kasha et al.[45,46] have coined the term 'solvent-cage perturbation of proton transfer spectroscopy' to demonstrate this fact. However, in micellar environments the solvent reorganization dynamics may be considerably slower compared to that in bulk homogeneous solvents.[19,27,33,35,47−49] It is evident from Table 2 that the shorter time component (*ca.* 1.6 ns) of the fluorescence transients characterizing the fluorescence lifetime of the neutral form of NHM gradually increases with the increasing micellar concentration. This observation may reflect the fact that solvent stabilized NHM molecules may encounter higher solvation energy barrier for the proton transfer process. This conjecture is in consensus with recent reports on the role of solvation on the excited-state proton transfer process in 1-naphthol.[47,48] Further, this is found to be in parity with previous results reported by Zewail et al.,[49] in which the competing processes of solvation and twisting dynamics were concluded to be the major deactivation pathways in the excited-state.

3.8. Rotational-Relaxation Dynamics. The time-resolved fluorescence anisotropy decay is expressed as[27]

$$r(t) = \sum_i r_{0i}\alpha_{ir} \exp(-t/\tau_{ir}) \quad (7)$$

where α_{ir} designates the pre-exponential factor for the ith rotational correlation time and τ_{ir}, $r_0 = \sum_i r_{0i}$ describes the limiting anisotropy.[27] Figure 11 illustrates the time-resolved fluorescence anisotropy decay of NHM in various environments under investigation and the rotational dynamic parameters are appended in Table 3.

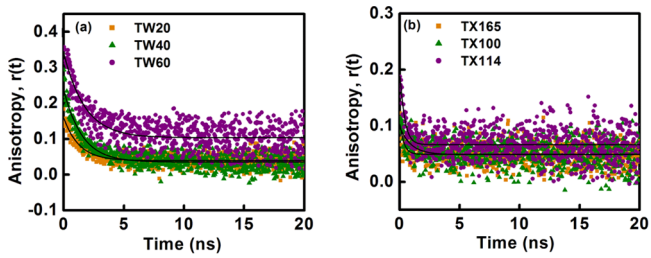

Figure 11. Time-resolved fluorescence anisotropy decay profile of the drug (NHM) in various micellar environments of (a) Tween series, and (b) Triton X series.

The anisotropy decay of NHM in aqueous buffer phase is found to be monoexponential in nature and is characterized by a rotational correlation time, $\tau_r \sim 132$ ps (Table 3). However, the rotational correlation time of NHM within the micelle-encapsulated state is found to be significantly enhanced implying the location of the drug molecules in motionally constrained environments (Table 3). It is interesting to note here that the anisotropy decay profiles of NHM within the micellar units are also described by monoexponential decay functions and the origin of the same may be argued based on the following rationales:[27,32,46,50]

(i) The exclusive rotation of the fluorophore within the micelles

dx.doi.org/10.1021/jp5056717 | J. Phys. Chem. B 2014, 118, 11209−11219

(ii) The micelle along with the fluorophore rotates with almost no independent and significant contribution from the fluorophore

(iii) Both the possibilities in parts i and ii are operational.

The attainment of a monoexponential anisotropy decay behavior readily rules out possibility iii as the situation necessitates a biexponential decay function to ensure an apt description. In order to resolve one of the two possibilities between points i and ii as mentioned above, the rotational correlation times of the micellar assemblies (τ_M) have been determined by applying the well-known Stokes−Einstein-Debye relationship:[27]

$$\tau_M = \frac{4}{3}\pi r_h^3 \times \frac{\eta}{k_B T} \quad (8)$$

Here, η is the coefficient of viscosity of the medium, r_h is the hydrodynamic radius of the micellar units (Table 3), k_B is the Boltzmann constant, T is the Kelvin temperature. The rotational-relaxation times of the micellar units (τ_M) are found to be markedly greater than the observed rotational correlation times of NHM in the respective micellar environments. This explicitly dictates that the rotational−relaxation dynamics of micelle-bound NHM is exclusively attributable to the rotational motion of the drug molecules with no significant contribution from the micellar rotation.[27,32,44−51]

4. CONCLUSIONS

In the present article, we have investigated the effect of variation in size of the headgroup and length of the alkyl chain of two series of nonionic surfactants, namely the Tween and Triton X on the interaction of a potent cancer cell photosensitzer NHM. We have conclusively proved that the binding of the drug molecule to the micellar aggregates is rather strong, spontaneous and our results have unraveled the intriguing modifications to the cation ⇌ neutral prototropic equilibrium of the drug as induced by the microheterogeneous micellar assemblies. Binding with the micellar assemblies is found to remarkably enhance the aforementioned prototropic equilibrium toward the neutral species over the cationic counterpart with the extent of the equilibrium being significantly influenced by the alkyl chain length (within the Tween series) or the PEO chain length (within the Triton X series).[51] Such differential modification to the photophysics of the drug molecule within the micelle-bound state has been attributed to the micellar hydration model that is, the differential degrees of water penetration to micellar units depending on the variation of the thickness of the palisade layer, which is the most probable location of NHM within the micellar units. The strength of drug-micelle binding (in terms of the binding constant (K) values) is also found to bear reasonable dependence on the alkyl chain length within the Tween series and PEO chain length within the Triton X series in a manner that it increases with increasing the alkyl chain length while decreases with an increase in the PEO chain length. Both steady-state and time-resolved fluorescence anisotropy results support the fact that the drug molecules experience significant motional rigidity within the micellar assemblies which is also found to increase with increasing alkyl chain length and decreasing PEO chain length.

■ ASSOCIATED CONTENT

Supporting Information

Steady-state and time-resolved spectral behavior of NHM as a function of medium pH and in the presence of surfactants and deconvolution of emission spectra of NHM under various experimental conditions. This material is available free of charge via the Internet at http://pubs.acs.org.

■ AUTHOR INFORMATION

Corresponding Authors

*E-mail: bpaul@iiserb.ac.in (B.K.P.).

*E-mail: saptarshi@iiserb.ac.in (S.M.).

Notes

The authors declare no competing financial interest.

■ ACKNOWLEDGMENTS

B.K.P. acknowledges IISER Bhopal for institute postdoctoral research fellowship and N.G. acknowledges CSIR, India, for a research fellowship. S.M. expresses thanks for the financial assistance from DST, India.

■ REFERENCES

(1) Rekharsky, M. V.; Inoue, Y. Complexation Thermodynamics of Cyclodextrins. *Chem. Rev.* **1998**, *98*, 1875−1917.

(2) Villalonga, R.; Cao, R.; Fragoso, A. Supramolecular Chemistry of Cyclodextrins in Enzyme Technology. *Chem. Rev.* **2007**, *107*, 3088−3116.

(3) Bodor, N. S. *Chemical Aspects of Drug Delivery Systems*; Karsa, D. R., Stephenson, R. A., Eds.; Royal Society of Chemistry: London, 1996.

(4) Xia, Y.; Rodgers, J.; Paul, K. E.; Whitesides, G. M. Unconventional Methods for Fabricating and Patterning Nanostructures. *Chem. Rev.* **1999**, *99*, 1823−1848.

(5) Hashimoto, S.; Thomas, J. K. Fluorescence Study of Pyrene and Naphthalene in Cyclodextrin-Amphiphile Complex Systems. *J. Am. Chem. Soc.* **1985**, *107*, 4655−4662.

(6) Paul, B. K.; Samanta, A.; Guchhait, N. Modulation of Excited-State Intramolecular Proton Transfer Reaction of 1-Hydroxy-2-naphthaldehyde in Different Supramolecular Assemblies. *Langmuir* **2010**, *26*, 3214−3224.

(7) Paul, B. K.; Samanta, A.; Guchhait, N. Exploring Hydrophobic Subdomain IIA of the Protein Bovine Serum Albumin in the Native, Intermediate, Unfolded, and Refolded States by a Small Fluorescence Molecular Reporter. *J. Phys. Chem. B* **2010**, *114*, 6183−6196.

(8) Tanford, C. The Hydrophobic Effect and the Organization of Living Matter. *Science* **1978**, *200*, 1012−1018.

(9) Kalyanasundram, K. *Photochemistry in Microheterogenous Systems*; Academic Press: New York, 1987.

(10) Rosen, M. J. *Surfactant and Interfacial Phenomena*; Wiley Interscience: New York, 1978.

(11) Fendler, H. J.; Fendler, J. E. *Catalysis in Micellar and Macromolecular Systems*; Academic:New York, 1975.

(12) Liveri, M. L. T.; Licciardi, M.; Sciascia, L.; Giammona, G.; Cavallaro, G. Peculiar Mechanism of Solubilization of a Sparingly Water Soluble Drug into Polymeric Micelles. Kinetic and Equilibrium Studies. *J. Phys. Chem. B* **2012**, *116*, 5037−5046.

(13) Kataoka, K.; Harada, A.; Nagasaki, Y. Block Copolymer Micelles for Drug Delivery: Design, Characterization and Biological Significance. *Adv. Drug Delivery Rev.* **2001**, *47*, 113−131.

(14) Bloom, H.; Barchas, J.; Sandler, M.; Usdin, E. *Progress in Clinical and Biological Research. β-carbolines and Tetrahydroisoquinolines*; Alan R. Liss Inc.; New York, 1982; Vol. *90*.

(15) Braestrup, C.; Nielsen, M.; Olsen, C. E. Urinary and Brain β-Carboline-3-carboxylates as Potent Inhibitors of Brain Benzodiazepine Receptors. *Proc. Natl. Acad. Sci. U.S.A.* **1980**, *77*, 2288−2292.

(16) Varela, A. P.; da G. Miguel, M.; Macanita, A. L.; Burrows, H. D.; Becker, R. S. β-Carboline Photosensitizers. 3. Studies on Ground and

Excited State Partitioning in AOT/water/cyclohexane Microemulsions. *J. Phys. Chem.* **1995**, *99*, 16093−16100.
(17) Dolmans, D. E.; Fukumura, D.; Jain, R. K. Photodynamic Therapy for Cancer. *Nature Rev. Cancer* **2003**, *3*, 380−387.
(18) Henderson, B., Dougherty, T., Eds. *Photodynamic Therapy: Basic Principles and Clinical Applications*; Marcel Dekker Inc.: New York, 1992.
(19) Reyman, D.; Pardo, A.; Poyato, J. M. L. Phototautomerism of β-Carboline. *J. Phys. Chem.* **1994**, *98*, 10408−10411.
(20) Beljanski, M.; Beljanski, M. S. Selective Inhibition of in Vitro Synthesis of Cancer DNA by Alkaloids of β-Carboline Class. *Exp. Cell Biol.* **1982**, *50*, 79−87.
(21) Dias, A.; Varela, A. P.; Miguel, M.; da, G.; Macanita, A. L.; Becker, R. S. Carboline Photosensitizers. 1. Photophysics, Kinetics and Excited-State Equilibria in Organic Solvents, and Theoretical Calculations. *J. Phys. Chem.* **1992**, *96*, 10290−10296.
(22) Paul, B. K.; Guchhait, N. Exploring the Strength, Mode, Dynamics, and Kinetics of Binding Interaction of a Cationic Biological Photosensitizer with DNA: Implication on Dissociation of the Drug-DNA Complex via Detergent Sequestration. *J. Phys. Chem. B* **2011**, *115*, 11938−11949.
(23) Becher, P. Nonionic surface-active compounds IV. Micelle Formation by Polyoxyethylene Alkanols and Alkyl Phenols in Aqueous Solution. *J. Colloid Sci.* **1961**, *16*, 49−56.
(24) Saito, Y.; Sato, T. Effects of Polyoxyethylene Chain Length on Micellar Structure. *J. Phys. Chem.* **1985**, *89*, 2110−2112.
(25) Partearroyo, M. A.; Alonso, A.; Goni, F. M.; Tribout, M.; Paredes, S. Solubilization of Phospholipid Bilayers by Surfactants Belonging to the Triton X Series: Effect of Polar Group Size. *J. Colloid Interface Sci.* **1996**, *178*, 156−159.
(26) Bevington, P. R.; Robinson, D. K. *Data Reduction and Error Analysis for the Physical Sciences*, 2nd ed.; WCB/McGraw-Hill: Boston, MA, 1992, Chapter 8.
(27) Lakowicz; J. R. *Principles of Fluorescence Spectroscopy*; Plenum: New York, 1999.
(28) O'Connor, D. V.; Philips, D. *Time Correlated Single Photon Counting*; Academic Press: London, 1984.
(29) Gonzalez, M. M.; Arnbjerg, J.; Denofrio, M. P.; Erra-Balsells, R.; Ogilby, P. R.; Cabrarizo, F. M. One- and Two-Photon Excitation of β-Carbolines in Aqueous Solution: pH-Dependent Spectroscopy, Photochemistry, and Photophysics. *J. Phys. Chem. A* **2009**, *113*, 6648−6656.
(30) Almgren, M.; Grieser, F.; Thomas, J. K. Dynamic and Static Aspects of Solubilization of Neutral Arenes in Ionic Micellar Solutions. *J. Am. Chem. Soc.* **1979**, *101*, 279−291.
(31) Paul, B. K.; Ray, D.; Guchhait, N. Binding Interaction and Rotational-Relaxation Dynamics of a Cancer Cell Photosensitizer with Various Micellar Assemblies. *J. Phys. Chem. B* **2012**, *116*, 9704−9717.
(32) Vazquez, M. E.; Blanco, J. B.; Imperiali, B. Photophysics and Biological Applications of the Environment-Sensitive Fluorophore 6-*N*,*N*-Dimethylamino-2,3-naphthalimide. *J. Am. Chem. Soc.* **2005**, *127*, 1300−1306.
(33) Reyman, D.; Viñas, M. H.; Poyato, J. M. L.; Pardo, A. Proton Transfer Dynamics of Norharman in Organic Solvents. *J. Phys. Chem. A* **1997**, *101*, 768−775.
(34) Tomas Vert, F.; Zabala Sanchez, I.; Olba Torrent, A. Acidity Constants of β-Carbolines in the Ground and Excited Singlet States. *J. Photochem.* **1983**, *23*, 355−368.
(35) Reyman, D.; Vinas, M. H.; Tardajos, G.; Mazario, E. The Impact of Dihydrogen Phosphate Anions on the Excited-State Proton Transfer of Harmane. Effect of β-Cyclodextrin on These Photoreactions. *J. Phys. Chem. A* **2012**, *116*, 207−214.
(36) Sytnik, A.; Kasha, M. Excited-State Intramolecular Proton Transfer as a Fluorescence Probe for Protein Binding-Site Static Polarity. *Proc. Natl. Acad. Sci. U.S.A.* **1994**, *91*, 8627−8630.
(37) Reichardt, C. Solvatochromic Dyes as Polarity Indicators. *Chem. Rev.* **1994**, *94*, 2319−2358.
(38) Karukstis, K. K.; D'Angelo, N. D.; Loftus, C. T. Using the Optical Probe Methyl Orange to Determine the Role of Surfactant and Alcohol Chain Length in the Association of 1-alkanols with Alkyltrimethylammonium Bromide Micelles. *J. Phys. Chem. B* **1997**, *101*, 1968−1973.
(39) Koswer, E. M. Reactions through Charge Transfer Complexes. In *Progress in Physical Organic Chemistry*, Taft, R. W., Ed.; Wiley Interscience: New York, 1965; Vol. 3.
(40) Muller, N. *Reaction Kinetics in Micelles* Cordes, E. A., Ed.; Plenum: New York, 1973.
(41) Berr, S.; Jones, R. R. M.; Johnson, J. S. Effect of Counterion on the Size and Charge of Alkyltrimethylammonium Halide Micelles as a Function of Chain Length and Concentration as Determined by Small-Angle Neutron Scattering. *J. Phys. Chem.* **1992**, *96*, 5611−5617.
(42) Robert, P. *Dynamic Light Scattering: Applications of Photon Correlation Spectroscopy*; Plenum: New York, 1985.
(43) Brown, W. *Light Scattering*; Oxford University Press: Oxford, U.K., 1996.
(44) Quitevis, E. L.; Marcus, A. H.; Fayer, M. D. Dynamics of Ionic Lipophilic Probes in Micelles: Picosecond Fluorescence Depolarization Measurements. *J. Phys. Chem.* **1993**, *97*, 5792−5769.
(45) Kasha, M. Proton-transfer Spectroscopy. Perturbation of the Tautomerization Potential. *J. Chem. Soc., Faraday Trans. 2* **1986**, *82*, 2379−2392.
(46) Kasha, M.; Sytnik, A.; Dellinger, B. Solvent Cage Spectroscopy. *Pure Appl. Chem.* **1993**, *65*, 1641−1646.
(47) Rakshit, S.; Saha, R.; Verma, P. K.; Pal, S. K. Role of Solvation Dynamics in Excited State Proton Transfer of 1-Naphthol in Nanoscopic Water Clusters Formed in a Hydrophobic Solvent. *Photochem. Photobiol.* **2012**, *88*, 851−859.
(48) Knochenmuss, R. D.; Smith, D. E. Time and Internal Energy Dependent Fluorescence Spectra of Naphthol-Water Clusters. *J. Chem. Phys.* **1994**, *101*, 7327−7336.
(49) Zhong, D.; Pal, S. K.; Zewail, A. H. Femtosecond Studies of Protein-DNA Binding and Dynamics: Histone I. *ChemPhysChem* **2001**, *2*, 219−227.
(50) Mukherjee, T. K.; Panda, D.; Datta, A. Excited-State Proton Transfer of 2-(2′-Pyridyl)benzimidazole in Microemulsions: Selective Enhancement and Slow Dynamics in Aerosol OT Reverse Micelles with an Aqueous Core. *J. Phys. Chem. B* **2005**, *109*, 18895−18901.
(51) Mahata, A.; Sarkar, D.; Bose, D.; Ghosh, D.; Girigoswami, A.; Das, P.; Chattopadhyay, N. Photophysics and Rotational Dynamics of a β-Carboline Analogue in Nonionic Micelles: Effect of Variation of Length of the Headgroup and the Tail of the Surfactant. *J. Phys. Chem. B* **2009**, *113*, 7517−7526.